Applied Microbiology and Biotechnology (2025) 109:67
https://doi.org/10.1007/s00253-025-13446-w

BIOENERGY AND BIOFUELS

Engineered *S. cerevisiae* construction for high-gravity ethanol production and targeted metabolomics

Peizhou Yang[1] · **Jiaqi Feng**[1] · **Jianchao Chen**[1]

Received: 14 June 2024 / Revised: 10 February 2025 / Accepted: 24 February 2025

Abstract

Strong sugar tolerance and high bioethanol yield of yeast under high-gravity fermentation have caused great attention in the bioethanol industry. In this study, Clustered Regularly Interspaced Short Palindromic Repeats Cas9 (CRISPR-Cas9) technology was used to knock out *S. cerevisiae GPD2*, *FPS1*, *ADH2*, *DLD3*, *ERG5*, *NTH1*, and *AMS1* to construct engineering strain *S. cerevisiae GFADENA*. Under high-gravity fermentation with 400 g/L of sucrose, *S. cerevisiae GFADENA* produced 135 g/L ethanol, which increased 17% compared with the wild-type strain. In addition, *S. cerevisiae GFADENA* produced 145 g/L of ethanol by simultaneous saccharification and fermentation (SSF) using 400 g/L of corn syrup with a sugar-ethanol conversion rate of 41.1%. Further, the targeted metabolomics involving energy, amino acid, and free fatty acid metabolisms were performed to unravel its molecular mechanisms. The deletion of seven genes in *S. cerevisiae GFADENA* caused a more significant effect on energy metabolism compared with amino acid and free fatty acid metabolisms based on the significantly different metabolites. Two metabolites α-ketoglutaric acid and fructose-1,6-bisphosphate were the most significantly different upregulation and downregulation metabolites, respectively ($p < 0.05$). Functions of metabolism, environmental information processing, and genetic information processing were related to sucrose tolerance enhancement and ethanol production increase in *S. cerevisiae GFADENA* by the regulation of significantly different metabolites. This study provided an effective pathway to increase ethanol yield and enhance sucrose tolerance in *S. cerevisiae* through bioengineering modification.

Key points

- *S. cerevisiae GFADENA with gene deletion was constructed by the CRISPR-Cas9 approach*
- *S. cerevisiae GFADENA could produce ethanol using high-gravity fermentation condition*
- *The ethanol yield of 145 g/L was produced using 400 g/L corn syrup by the SSF method*

Keywords *Saccharomyces cerevisiae* · Targeted metabolomics · High-gravity fermentation · Ethanol production · CRISPR-Cas9 approach

Introduction

Saccharomyces cerevisiae was one of the important cell factories that consume sucrose to produce bioethanol due to its robustness, genetic accessibility, and stress tolerance (Gombert and van Maris 2015; Marques et al. 2016). In industrialized large-scale fermentation systems, high-gravity fermentation was an effective approach to increase production capacity and reduce costs (Randez-Gil et al. 1999). However, high-gravity sucrose alcohol fermentation caused severe disadvantage effects including yeast cell shrinkage, cell vitality, and even death (Verstrepen et al. 2004). The stress tolerance improvement of yeast to sucrose was of great significance for bioethanol production under the condition of high gravity by constructing

✉ Peizhou Yang
yangpeizhou@hfut.edu.cn

Jiaqi Feng
fengjqi@126.com

Jianchao Chen
cjc183030@163.com

[1] School of Food and Biological Engineering, Anhui Province Key Laboratory of Agricultural Products Modern Processing, Hefei University of Technology, Feicui Road 420, Shushan District, Hefei 230601, China

Published online: 19 March 2025

engineered strains (van Aalst et al. 2022). In addition, the modification of glucose to the ethanol metabolism pathway by the gene editing approach was an effective means to improve ethanol yield.

Genetic modification affects yeast's tolerance to the environment by increasing or decreasing the accumulation of specific products. The stress tolerance of yeast was directly affected by cell wall and membrane defense systems, which were composed of a matrix of extracellular polymeric substances including ergosterol, trehalose, and mannan by respectively knocking out *ERG5*, *NTH1*, and *Ams1* genes (Flemming and Wingender 2010; Wu et al. 2023). The deletion of *S. cerevisiae ERG5* resulted in significant resistance improvement to external stresses by accumulating an intermediate product fecosterol during the sterol biosynthesis pathway (Caspeta et al. 2014; Lam et al. 2014). Trehalose prevented protein denaturation via hydrogen bridges to the polar residues of protein (Crowe et al. 1998). The inhibition of trehalase *NTH1* enhanced the yeast stress resistance by modifying the trehalose hydrolysis pathway (Nwaka et al. 1995). α-Mannosidase Ams1 played a role in the catabolism degradation of N-linked free mannose oligosaccharides (Umekawa et al. 2016). In addition, *Ams1* deletion reduced the further decomposition efficiency of mannan, leading to the accumulation of mannan (Hirayama and Suzuki 2011; Trimble and Atkinson 1992).

The ethanol production of *S. cerevisiae* was improved by the deletion of *GPD2*, *Fps1*, and *DLD3* (Hubmann et al. 2011). *S. cerevisiae GPD2* was an isoform of glycerol 3-phosphate dehydrogenase (GPDH) with a function as a rate-controlling enzyme of glycerol formation. The Fps1 glycerol channel in *S. cerevisiae* was a member of the major intrinsic protein family. Fps1 functioned to transport glycerol passively out of the strain cell in osmoregulatory pathways (Beese-Sims et al. 2011). The deletion of the alcohol dehydrogenase isozyme *ADH2* reduced the formation of acetaldehyde and fuel alcohols (Wu et al. 2021). The downregulation of *D*-lactate dehydrogenase gene *(DLD3*) resulted in ethanol tolerant enhancement and higher ethanol production (Kim et al. 2011).

In this study, seven genes of *GPD2*, *FPS1*, *ADH2*, *DLD3*, *ERG5*, *NTH1*, and *AMS1* were knocked out to increase the ethanol yield and tolerance to sucrose by the Clustered Regularly Interspaced Short Palindromic Repeats Cas9 (CRISPR-Cas9) approach (Fig. 1A). The effect of gene deletion on the ethanol yield of yeast was investigated. The stress tolerance of engineered yeast was also analyzed using high-gravity sucrose. In addition, the molecular mechanism of the *S. cerevisiae* mutant was further explored based on the targeted metabolomics of energy, amino acid, and free fatty acid metabolisms.

Materials and methods

Strains, chemicals, and reagents

S. cerevisiae used in this study for genetic modification was haploid yeast (ATCC® 204,508™). All the engineering strains have been deposited in the Anhui Province Key Laboratory of Agricultural Products Modern Processing (Hefei, China). The collection number of engineering *S. cerevisiae GFADENA* is No. 2022171602. The determination of metabolites and data analysis of the targeted metabolomics were performed by Personalbio Company (China, Nanjing). Acetonitrile (ACN) and methanol (MeOH) were from Merck (Darmstadt, Germany). The sucrose sample was from Olchemlm Ltd. (Olomouc, Czech Republic). The stock solution of the standard sample was prepared by dissolving the sample in 1 mg/mL of MeOH. Phusion High-Fidelity PCR Master Mix with HF Buffer for polymerase chain reaction (PCR) amplification was from New England Biolabs Company (NEB). High-performance liquid chromatography (HPLC) equipment (Waters series high-performance liquid chromatography) equipped with differential refractive index detector (RID) and Sugar SH1011.

Measurement of sucrose, glucose, and ethanol concentrations

The HPLC approach was used to determine the concentrations of sucrose, glucose, and ethanol according to previously reported methods (El-Sheekh et al. 2022; Gombert and van Maris 2015). HPLC determination conditions were prepared using 0.01 mol/L of H_2SO_4 with a mobile phase, flow rate of 0.8 mL/min, and column temperature set at internal 35 °C and external 50 °C. Each sample had an injection volume of 10 µL and was set for 25 min.

gRNA expression vector design and transformation method

The 23-bp guide RNA of each gene was selected to amplify the expression vectors for gene recognition using online Web link http://chopchop.cbu.uib.no/ (Montague et al. 2014). The primers of gRNA expression vector amplification including *GPD2*, *FPS1*, *ADH2*, *DLD3*, *ERG5*, *NTH1*, and *AMS1* gRNA using gRNA-trp-HyB plasmid as a template are listed in Table 1. The reaction system was prepared by 12.5 µL Phusion Master Mix, 0.5 µM forward primer, 0.5 µM reverse primer, 0.5 µL template, and 10 µL sterile double distilled water. The reaction run using the amplification parameters of 98 °C heating for 30 s; 98 °C denaturation for 8 s, 50 °C annealing for 25 s, 72 °C extension for 3 min for 29 cycles;

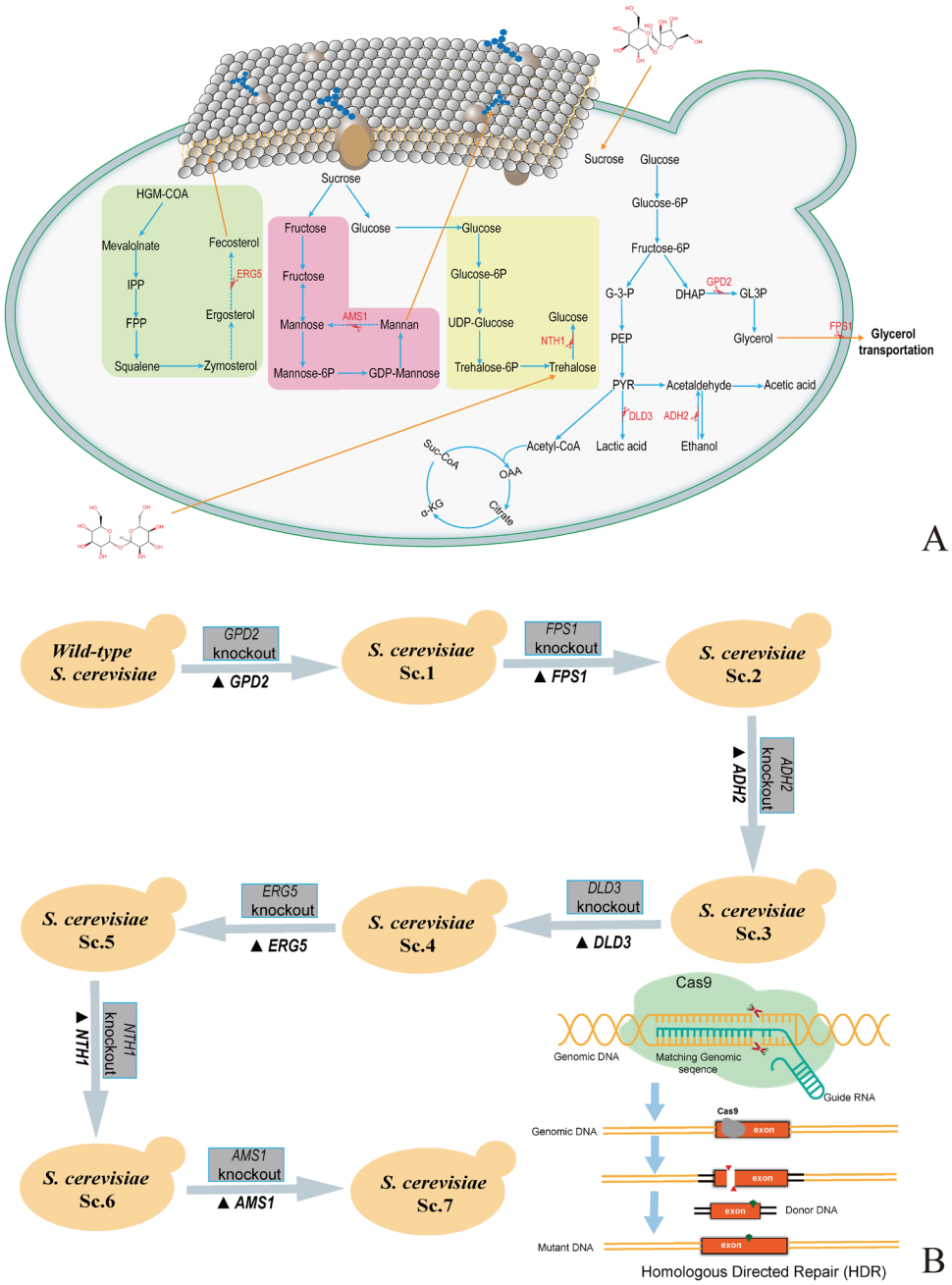

Fig. 1 Construction strategy and technical pathway of *S. cerevisiae GFADENA* in this study. Note: **A** Construction strategy of engineered strains to increase the yield of ethanol and enhance the tolerance of sucrose by the CRISPR-Cas9 approach by the deletion of *S. cerevisiae GPD2*, *FPS1*, *ADH2*, *DLD3*, *ERG5*, *NTH1*, and *AMS1*. **B** Technical pathway of *S. cerevisiae GFADENA* construction by the sequential deletion of *S. cerevisiae GPD2*, *FPS1*, *ADH2*, *DLD3*, *ERG5*, *NTH1*, and *AMS1* in this study. *S. cerevisiae GFADENA* meant engineered *S. cerevisiae* strain after the deletion of *GPD2*, *FPS1*, *ADH2*, *DLD3*, *ERG5*, *NTH1*, and *AMS1*. The figure in the lower right corner represents the technical principle of gene editing by the CRISPR-Cas9 approach to knock out specific genes in yeast

and 72 °C for 5 min. The genetic transformation of *S. cerevisiae* was performed according to the PEG-mediated transformation method (Gietz and Schiestl 2007).

Engineered *S. cerevisiae* mutant construction

The gene deletion of *S. cerevisiae* was implemented by the CRISPR-Cas9 technology. After the transformation of double-vector transformation of the Cas9-NAT plasmid and the gRNA vector, the insert fragments were integrated into the yeast genome specified by gRNA to achieve knockout of the target gene. The solid screening media for Cas9-NAT plasmid and the gRNA vector transformation were prepared by YPD solid media containing 80 μg/mL nourseothricin and 300 μg/mL hygromycin B, respectively. Through multiple rounds of transformation, screening, and identification, the final engineered *S. cerevisiae* was constructed with the deletion of *GPD2*, *FPS1*, *ADH2*, *DLD3*, *ERG5*, *NTH1*, and *AMS1* genes (Fig. 1B).

Resistance stress investigation on the solid sucrose medium

The YP culture media were prepared with 10 g/L yeast extract, 20 g/L peptone, and sucrose as a carbon source for

Table 1 Primers for gRNA vector amplification and PCR identification of the corresponding insertion DNA

Primers	Sequences
GPD2-gRNA-F1	TGATTGGTTCTGGTAACTGGGGGGTTTTAGAGCTAGAAATAGCAAG
GPD2-gRNA-R1	CCCCCAGTTACCAGAACCAATCAGATCATTTATCTTTCACTGCGGA
Us/Ds-TV-AFB1D	*5′-ATGGCTCGCGCGAAGTACTC-3′/5′-TTAAAGCTTCCGCTCTATGAA-3′*
Fps1-gRNA-F1	AATAAGCAGTCATCCGACGAAGGGTTTTAGAGCTAGAAATAGCAAG
Fps1-gRNA-R1	CCTTCGTCGGATGACTGCTTATTGATCATTTATCTTTCACTGCGGA
Us/Ds–OM-PLA1	*5′-TATGCGCATTTTGTCAGGGA-3′/5′-GATTACATAATATCGTTCAGC-3*
ADH2-gRNA-F1	GGAAACATTGATGATACCGTGGGGTTTTAGAGCTAGAAATAGCAAG
ADH2-gRNA-R1	CCCACGGTATCATCAATGTTTCCGATCATTTATCTTTCACTGCGGA
Us/Ds-DPE	*5′-CAGAAAAGCGAAAGAGACACC-3′/5′-TGAGGATATTATCGCAAATC-3*
DLD3-gRNA-F	TTGGCAGTAGTACCACAAGGTGGGTTTTAGAGCTAGAAATAGCAAG
DLD3-gRNA-R	CCACCTTGTGGTACTACTGCCAAGATCATTTATCTTTCACTGCGGA
L1-F/L1-R	*5′-ATGAATACATATCACCCATTCAG-3′/5′-TTATGCCTCCTTCATTCCG-3′ 640 bp*
ERG5-gRNA-F	ATTTCATGGAAAAAGACCTGGGGGTTTTAGAGCTAGAAATAGCAAG
ERG5-gRNA-R	CCCCAGGTCTTTTTCCATGAAATGATCATTTATCTTTCACTGCGGA
L1-F/L1-R	*5′-ATGAATACATATCACCCATTCAG-3′/5′-TTATGCCTCCTTCATTCCG-3′*
NTH1-gRNA-F	TTAAATAACCATAAGAACGGAGGGTTTTAGAGCTAGAAATAGCAAG
NTH1-gRNA-R	CCTCCGTTCTTATGGTTATTTAAGATCATTTATCTTTCACTGCGGA
C-F/C1-R	*5′-ATGAGTTCAAATAAACTGACAACTAG-3′/5′-GATATTTAATCCATACGCCT-3′*
AMS1-gRNA-F	GATATCACTCAATGCAACTGCGGGTTTTAGAGCTAGAAATAGCAAG
AMS1-gRNA-R	CCGCAGTTGCATTGAGTGATATCGATCATTTATCTTTCACTGCGGA
C-F/C2-R	*5′-ATGAGTTCAAATAAACTGACAACTAG-3′/5′-TTAAGAATCTTTTTTAATCGG-3′*

Primers of *GPD2*-gRNA-F1/*GPD2*-gRNA-R1, Fps1-gRNA-F1/Fps1-gRNA-R1, *ADH2*-gRNA-F1/*ADH2*-gRNA-R1, *DLD3*-gRNA-F/*DLD3*-gRNA-R, *ERG5*-gRNA-F/*ERG5*-gRNA-R, *NTH1*-gRNA-F/*NTH1*-gRNA-R, and *AMS1*-gRNA-F/*AMS1*-gRNA-R were used to construct *GPD2*-gRNA, *FPS1*-gRNA, *ADH2*-gRNA, *DLD3*-gRNA, *ERG5*-gRNA, *NTH1*-gRNA, and *AMS1*-gRNA expression vectors, respectively. In addition, the italicized *Us/Ds-TV-AFB1D*, *Us/Ds–OM-PLA1*, *Us/Ds-DPE*, *L1-F/L1-R*, *L1-F/L1-R*, *C-F/C1-R*, and *C-F/C2-R* primers were used to identify the corresponding insertion DNA

resistance investigation. The specific operation processes were as follows: (1) the yeast fermentation solution of 5 μL spotted on the solid medium containing high-concentration sucrose for resistance stress investigation. The initial cell concentration of yeast for the test was quantified to 5 OD_{600nm}; (2) then, the different strain spots were sequentially diluted for investigation by the gradient dilution ten times on the sucrose concentrations of 100, 200, 300, and 400 g/L. The effect of incubation time on the growth of engineered *S. cerevisiae* was investigated on the solid sucrose medium at 30 °C. The cell proliferation of yeast on the solid plate was assessed according to the diameter sizes of colony circles.

Calculation equation between yeast cell density and its dry weight

The calculation equation between yeast cell density and its dry weight was determined based on the optical density (OD) values at the wavelength of 600 nm and its corresponding cell dry weight. The chart was drawn according to the relation between cell weight and OD_{600nm} values. The horizontal and vertical axes represented cell dry weight (g/L) and OD_{600nm} values, respectively. The equation between OD_{600nm} values and cell dry weight was formulated based on data simulation. Then, this equation was used to calculate the cell dry weight according to OD_{600nm} values.

Effect of sucrose concentrations on the ethanol yields

The liquid fermentation medium was prepared by YP culture solution containing 10 g/L yeast extract, 20 g/L peptone, and a certain concentration of sucrose. The effect of sucrose concentrations on cell proliferation was investigated according to the OD_{600nm} values at the wavelength of 600 nm (Yang et al. 2023). The dry cell weight was calculated according to the equation of the relationship between cell weight and OD values at the wavelength of 600 nm (Wang et al. 2010). The volume of 2 mL fermentation solution with 5 OD_{600nm} was added to a 250-mL conical flask equipped with 100 mL of fermentation solution. The cell proliferation and ethanol yield of engineering yeast were investigated during the fermentation of 72 h using the wild-type strain as the control.

Simultaneous saccharification and fermentation of corn by *S. cerevisiae* GFADENA

Simultaneous saccharification and ethanol fermentation of corn were implemented as the following steps. (1) Corn was crushed into particles with a size of 2–3 mm diameter. (2) Mixing materials: clear liquid, distilled water, and tower kettle water (12:73:15, w/w/w) were added into 1-L glass reactor; then, corn powder was added into the reactor at 27% of liquid volume (w/v); material mixture was adjusted to pH 6 at 70 °C; α-amylase was added with 0.267 kg per ton of dry material and mixed at 67 °C for 40 min with a shaking speed of 120 rpm. (3) Liquefaction: the reaction kettle was placed in a water bath of 90 °C, with a mixing speed of 80 rpm for 2 h. After liquefaction, the reaction was cooled down to 32 °C for packaging. (4) Simultaneous saccharification and fermentation were performed in a 1000-mL conical flask equipped with 200 g of liquefaction by diluting with water to 500 mL. The final corn syrup concentration was 400 g/L for fermentation. The mixture solution contained saccharifying enzyme (0.727 kg/1000 kg), acid protease (0.035 kg/1000 kg), urea (1.5 kg/1000 kg), and yeast (0.05%, w/w). The tube was sealed with paraffin solution and incubated in a shaking bed with a shaking speed of 100 rpm at 32 °C. After fermentation, the mature mash was processed for further analysis.

Sample preparation for metabolomics detection

The yeast cells were cultured in the YPD liquid medium at 30 °C with a shaking speed of 150 rpm after 96 h of inoculation. The cells of yeast were collected in centrifuge tubes by centrifugation at 3000 rpm for 3 min after 0, 48, and 96 h of fermentation. Then, the yeast cells were evenly mixed using 5 mL of quenching solution prepared with the solution containing methanol–acetonitrile-water of 2:2:1 (v/v/v). The extraction solution (methanol-chloroform-water of 2:2:1, v/v/v) and equal volumes of SiO_2 beads were added to freezing and thawing cells with liquid nitrogen. During the preparation of intracellular products, the sample was placed in ice to ensure the stability of metabolites. The yeast cell lysate was treated at 4 °C after centrifugation at 12,000 rpm for 5 min. The supernatant was collected and dried with N_2 at room temperature. The solid powder was dissolved in 0.5 mL of extraction solution (acetonitrile–water of 1:1, v/v) at − 20 °C. After a centrifugation of 12,000 rpm for 5 min at 4 °C, the collected supernatant was dried with N_2 and frozen at − 80 °C. Finally, the samples were dissolved in 200 µL solution (acetonitrile–water of 7:3, v/v) for UPLC-Q-TOF/MS and LC–MS/MS detection.

Targeted metabolomics based on the quantitative analysis of metabolites

The targeted metabolomics were analyzed to unveil the molecular mechanism of engineered *S. cerevisiae* based on energy, free fatty acid, and amino acid metabolisms. The operation processes included sample collection, metabolite extraction, mass spectrometry analysis, data processing, metabolite annotation, data interpretation, and functional analysis (Gold et al. 2015). *S. cerevisiae* cell preparation and extraction were performed by the acetonitrile/methanol treatment technique. The extracted products were analyzed using an LC–ESI–MS/MS system (www.waters.com/nextgen/us/en. https://sciex.com/). HPLC analysis required a column of ACQUITY UPLC BEH Amide (2.1 mm × 100 mm × 1.7 µm); water solvent system prepared by 10 mM ammonium acetate and 0.3% ammonium hydroxide (v/v) (A), 90% acetonitrile/water (v/v) (B); flow rate of 0.4 mL/min; and temperature of 40 °C.

ESI–MS/MS treatment conditions

Linear ion trap and triple quadrupole scans were acquired on a triple quadrupole-linear ion trap mass spectrometer equipped with an ESI Turbo IonSpray interface controlled by Analyst 1.6.3 software (Kim et al. 2007). The ESI parameters were ion source of ESI ±, source temperature of 550 °C, ion spray voltage, and curtain gas of 35 psi (high-purity Helium). Tryptophan and metabolites were analyzed using the scheduled multiple-reaction monitoring. Data acquisitions and Sciex Multiquant 3.0.3 software were performed using Sciex Software Analyst 1.6.3 and quantified metabolites, respectively. Mass spectrometer parameters of the declustering potentials and collision energies for individual MRM transitions were performed with further optimization. MRM transitions were monitored for each period according to the eluted metabolites.

Data treatment for metabolomics analysis

Unsupervised principal component analysis (PCA) was performed by statistics function prcomp within *R* using online www.r-project.org (Girelli et al. 2023). The hierarchical cluster analysis (HCA) results were presented as heatmaps with dendrograms. Pearson correlation coefficients (PCC) between samples were calculated by the function in *R* and presented as only heatmaps. The original contents of differential metabolites identified by screening criteria by row using unit variance scaling (UV scaling) were normalized to facilitate the observation of changes in metabolite content. The heatmap was drawn using the R software package. Normalized signal intensities of metabolites for HCA were visualized as a color spectrum. Significantly regulated

metabolites were determined by corrected *p*-value and absolute Log_2FC (fold change). KEGG compound database (http://www.kegg.jp/kegg/compound/) was used to identify metabolites and annotate using annotated metabolites (http://www.kegg.jp/kegg/pathway.html). Pathways of significantly regulated metabolites mapped were fed into metabolite sets enrichment analysis (MSEA). The significance was determined by the hypergeometric test's *p*-values.

Metabolite annotation, data interpretation, and functional analysis

The targeted metabolomics from energy, energy, free fatty acid, and amino acid metabolisms of engineered *S. cerevisiae* was conducted using the quantitative analysis of metabolites based on the LC–MS/MS platform. Partial Least Squares Discriminant Analysis (PLS-DA) using supervised pattern recognition was used to screen differential metabolites. When the Variable Importance in Projection (VIP) of contemporary metabolites was greater than or equal to 1, a significantly differential metabolite was considered. The *p*-value or fold change of univariate analysis was combined to screen the differential metabolites. When fold change was greater than or equal to 1.2 and fold change was less than or equal to 0.8334, the difference was statistically significant at the level of $p < 0.05$. Due to the large number of variables in metabolomics, multiple hypothesis testing was used to correct for *p*-values and reduce false positives. KEGG was used to annotate significantly different metabolites. The annotation results were classified according to the pathway types in KEGG.

Data treatment and software analysis

All the data obtained from three repeated experiments were given as means ± standard deviation (*S.D.*). The statistics of data were analyzed using Software OriginPro 2018. Three biological replicates after 0, 48, and 96 h of fermentation were set up with six technical replicates for metabolomics experiment.

Results

Engineered *S. cerevisiae* construction using the CRISPR-Cas9 approach

Engineered *S. cerevisiae GFADENA* was constructed by successively knocking out *GPD2*, *FPS1*, *ADH2*, *DLD3*, *ERG5*, *NTH1*, and *AMS1* genes using the CRISPR-Cas9 approach. The screening of the putative transformants was performed on the YPD solid screening media after the transformation of gRNA expression and Cas9 vectors (Fig. 2A). A total of 15 colonies grew on the solid screening media with no colony on the plates from the three control groups. The putative transformants were further confirmed by amplifying and sequencing insertion DNA. The true transformants were used for further research.

Tolerance test of *S. cerevisiae* GFADENA on the solid sucrose medium

S. cerevisiae GFADENA grew on the solid YP media containing sucrose with the wild-type strain as the control. *S. cerevisiae GFADENA* had a similar growth with the wild-type strain under the low sucrose concentrations of 100 g/L (Fig. 2B–(A)). *S. cerevisiae GFADENA* possessed a better growth rate than the wild-type strain on the solid media containing high-concentration sucrose of 200–400 g/L (Fig. 2B–(B, C, and D)). Thus, *S. cerevisiae GFADENA* after *GPD2*, *FPS1*, *ADH2*, *DLD3*, *ERG5*, *NTH1*, and *AMS1* deletion obtained higher sucrose resistance under the high-concentration condition than the wild-type strain.

Effect of fermentation time on dry cell weight of *S. cerevisiae* GFADENA

The dry cell weights (DCW) of *S. cerevisiae GFADENA* were calculated according to the equation between DCW and OD values of *S. cerevisiae GFADENA*. The conversion formula was $y = 2.3045x + 0.1421 (R^2 = 0.9973)$, in which *y* and *x* represented OD_{600nm} values and cell weight concentrations (g/L), respectively (Fig. 2C). *S. cerevisiae GFADENA* had a faster growth rate during the initial 30-h fermentation than the wild-type strain under the liquid fermentation of 400 g/L sucrose. DCW of engineered *S. cerevisiae GFADENA* after fermentation of 18 h (1.56 g/L) was 17 folds than the control (0.09 g/L). The cell yields of *S. cerevisiae GFADENA* after fermentation of 48 h (3.51 g/L) were 1.08 folds compared with that of the wild-type strain (3.26 g/L) (Fig. 2D). Thus, engineered *S. cerevisiae GFADENA* possessed a faster cell proliferation rate than the control under the condition of high-concentration sucrose.

Effect of fermentation time on sucrose consumption and ethanol production

Sucrose concentrations and ethanol production were determined using 400 g/L of sucrose as fermentation substrate during the fermentation of 96 h (Fig. 3A). The ethanol concentration of *S. cerevisiae GFADENA* (135 g/L) was 1.17 folds than that of the wild-type strain (115 g/L). The residual sucrose content of *S. cerevisiae GFADENA* was higher than the wild-type strain. In addition, the concentration of glycerol in *S. cerevisiae GFADENA* was

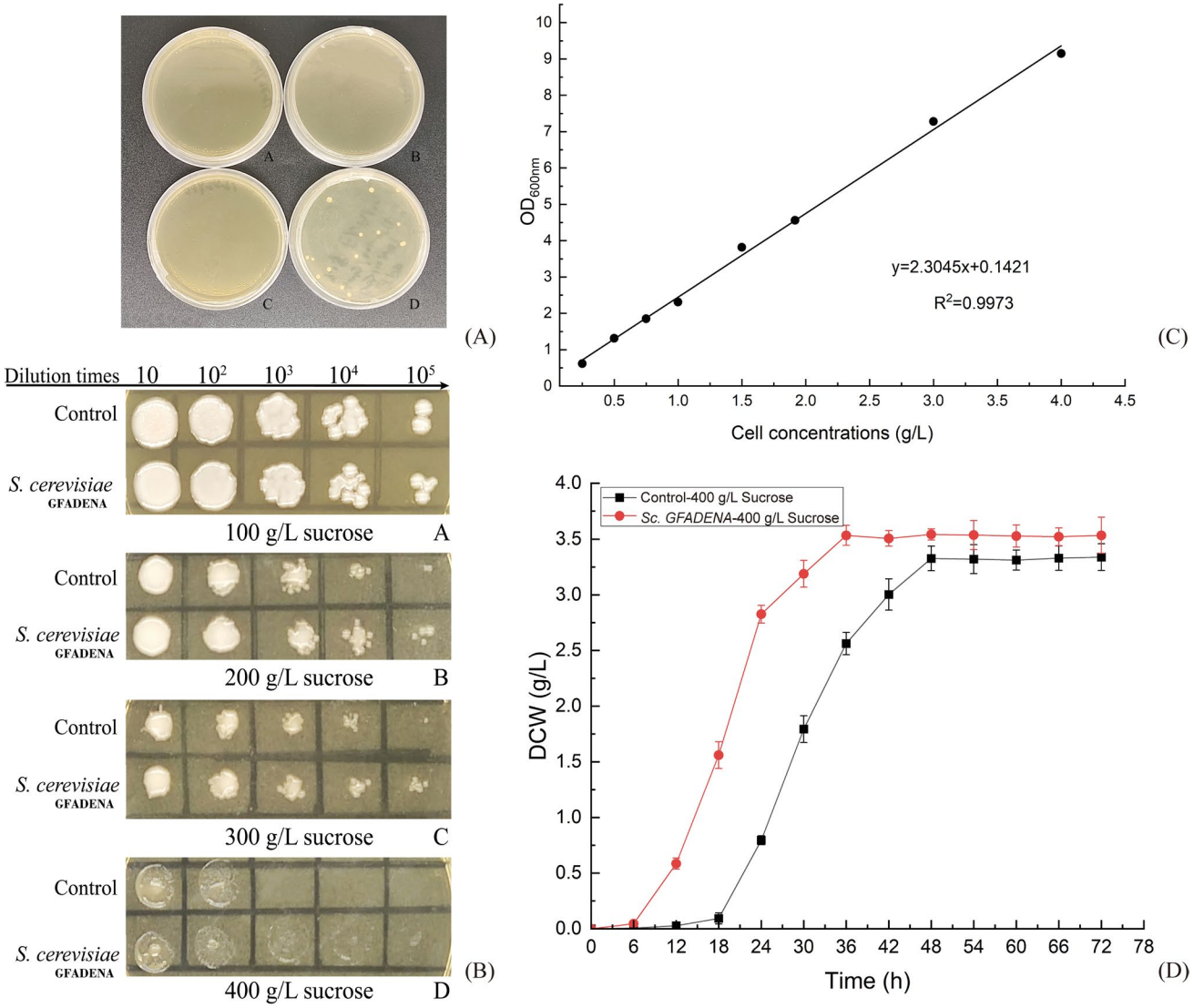

Fig. 2 Screening of the putative transformants and growth of *S. cerevisiae GFADENA* using 400 g/L of sucrose. Note: **A** The screening of putative transformants on the YPD solid media containing dual antibiotics. **A**, **B** The plate after the transformation without gRNA expression vector and insertion DNA, respectively. **C** The culture of yeast strain containing Cas expression vector by the direct coating plate without transformation. **D** The normal transformation for targeted gene deletion; **B** the cell growth of *S. cerevisiae GFADENA* on the solid YP sucrose media. Note: A, B, C, and D indicate the cell growth on the media containing sucrose concentrations of 100, 200, 300, and 400 g/L with the wild-type strain as the control, respectively; **C** the equation between cell concentrations (g/L) and OD values at the wavelength of 600 nm (OD_{600nm}); **D** the dry cell weights of *S. cerevisiae GFADENA* (g/L) during the fermentation using 400 g/L of sucrose with the wild-type strain as the control

9.21 g/L, which was 0.63 folds compared to the control yeast (14.53 g/L) after fermentation of 72 h under 400 g/L sucrose (Fig. 3B). The engineering yeast produced a certain amount of glycerol. Nevertheless, the glycerol content of engineering yeast had remarkably decreased compared to the control strain. Thus, *S. cerevisiae GFADENA* had stronger sucrose consumption capability and higher ethanol production efficiency than the wild-type strain.

Ethanol production of *S. cerevisiae* GFADENA using high-gravity corn syrup

S. cerevisiae GFADENA was applied to produce ethanol using 400 g/L of corn syrup. *S. cerevisiae GFADENA* could effectively produce ethanol with the highest ethanol concentration of 145 g/L after fermentation for 66 h during the fermentation of 96 h (Fig. 3C). The conversion efficiency of sugar to ethanol was 2.2 g/L/h based on the calculation of

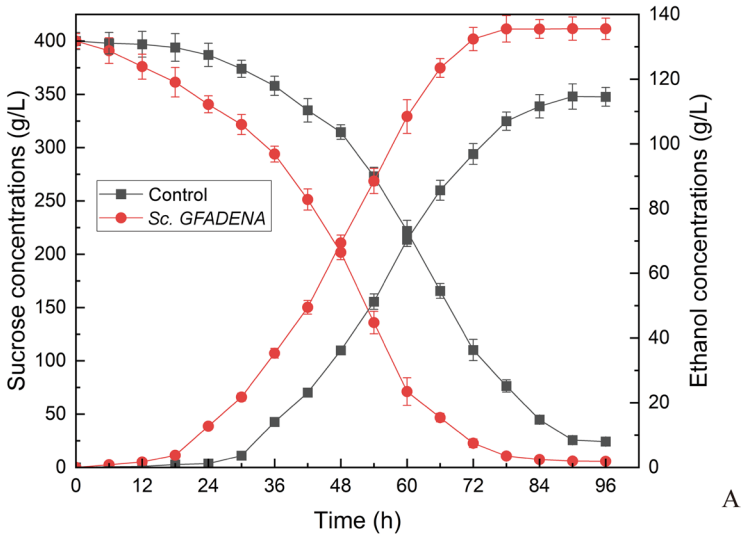

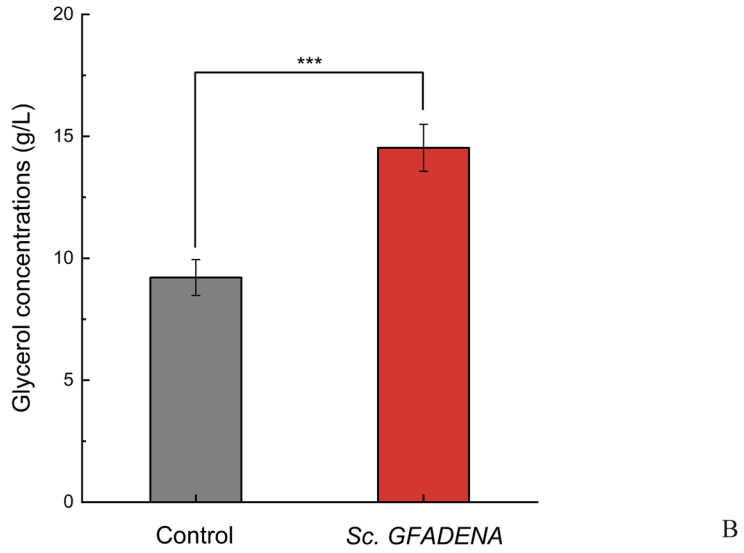

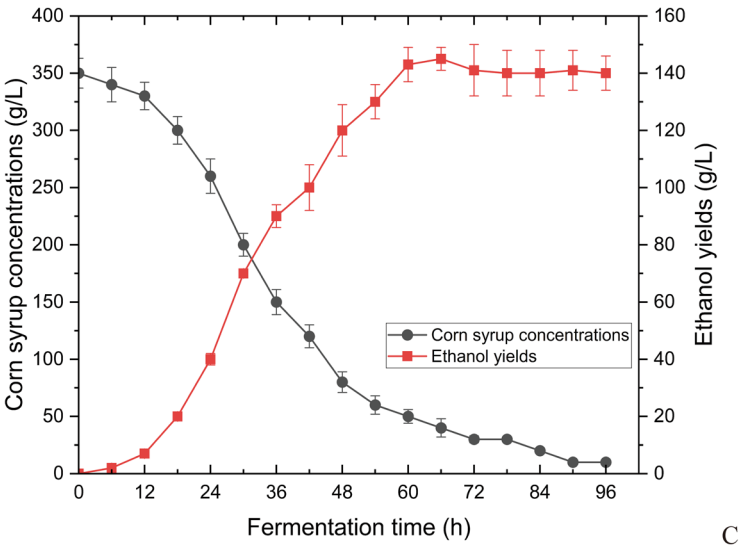

Fig. 3 Ethanol concentrations of *S. cerevisiae GFADENA* using sucrose and corn syrup. Note: **A** Sucrose and ethanol concentrations of *S. cerevisiae GFADENA* during the fermentation using sucrose as a carbon source. **B** Glycerol concentrations of *S. cerevisiae GFADENA* and the control after fermentation of 72 h under 400 g/L sucrose. **C** Ethanol yields and corn syrup concentrations during the fermentation of *S. cerevisiae GFADENA* by the simultaneous saccharification and fermentation approach

ethanol conversion rate and fermentation time. The conversion rate from glucose to ethanol in *S. cerevisiae GFADENA* reached 41.1%. The rate accounted for 81% of the theoretical conversion rate (51.1%). After fermentation for 96 h, the concentration of corn syrup was 10 g/L. The utilization rate of corn syrup reached 97%. Thus, *S. cerevisiae GFADENA* possessed excellent high-sugar tolerance and ethanol conversion ability.

Principal component analysis (PCA) based on targeted metabolomics of energy metabolism

The determination data of index, compounds, and class based on energy sigMetabolites are listed in Table S1. PCA modeling method was used to analyze the two sets of measured data to distinguish the significant differences between *S. cerevisiae GFADENA* and the wild-type strain. The PC1 and PC2 contribution rates under the cumulative condition of 99.32% were 96.52% and 2.8%, respectively (Fig. 4A). No significant difference existed between the two metabolome groups by two-dimensional principal component score plots ($p < 0.05$) (Fig. 4B). A significant difference existed between the two groups based on the scores of the predicted principal components ($p < 0.05$) (Fig. 4C). An aggregation interval existed significant differences between *S. cerevisiae GFADENA* and the wild-type strain. The formulas of validated OPLS-DA models were $R^2X = 0.947$, $R^2Y = 0.996$, and $Q^2 = 0.978$ ($p < 0.005$) by the data analysis from 200 random permutations (Fig. 4D).

Differential metabolites between *S. cerevisiae* GFADENA and the wild-type strain

The classification of metabolites was figured out between *S. cerevisiae GFADENA* and the wild-type strain (Fig. 5A). The differential metabolite *L*-cystine,

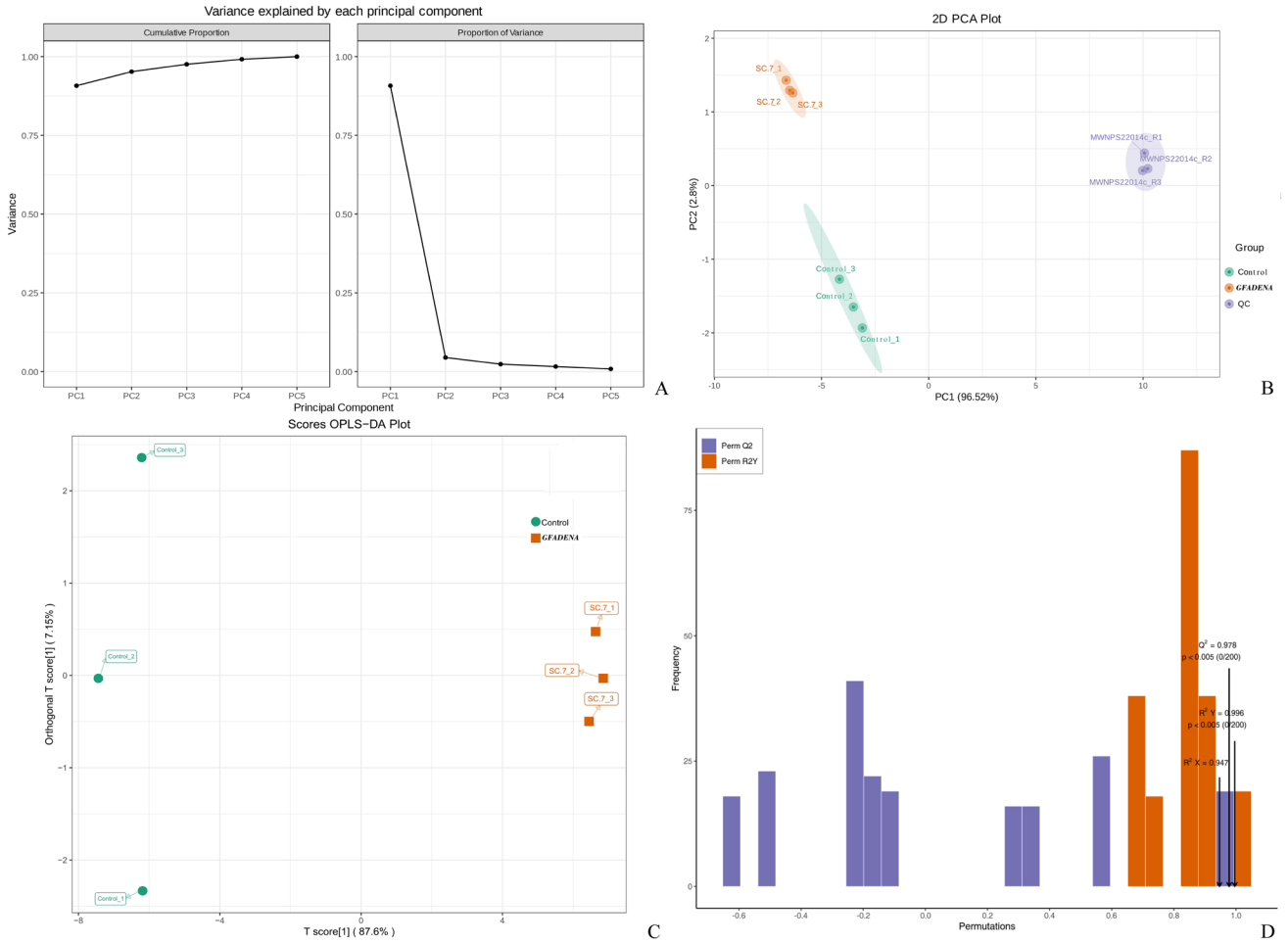

Fig. 4 Principal component analysis (PCA) of *S. cerevisiae GFADENA*. Note: **A** Variability of the data between PC1 and PC2; **B** difference between the metabolomes by the two-dimensional principal component score plots; **C** significant difference of *S. cerevisiae GFADENA* between the metabolomes of the two groups according to the scores of the predicted principal components; **D** validated OPLS-DA models by the data analysis of 200 random permutations

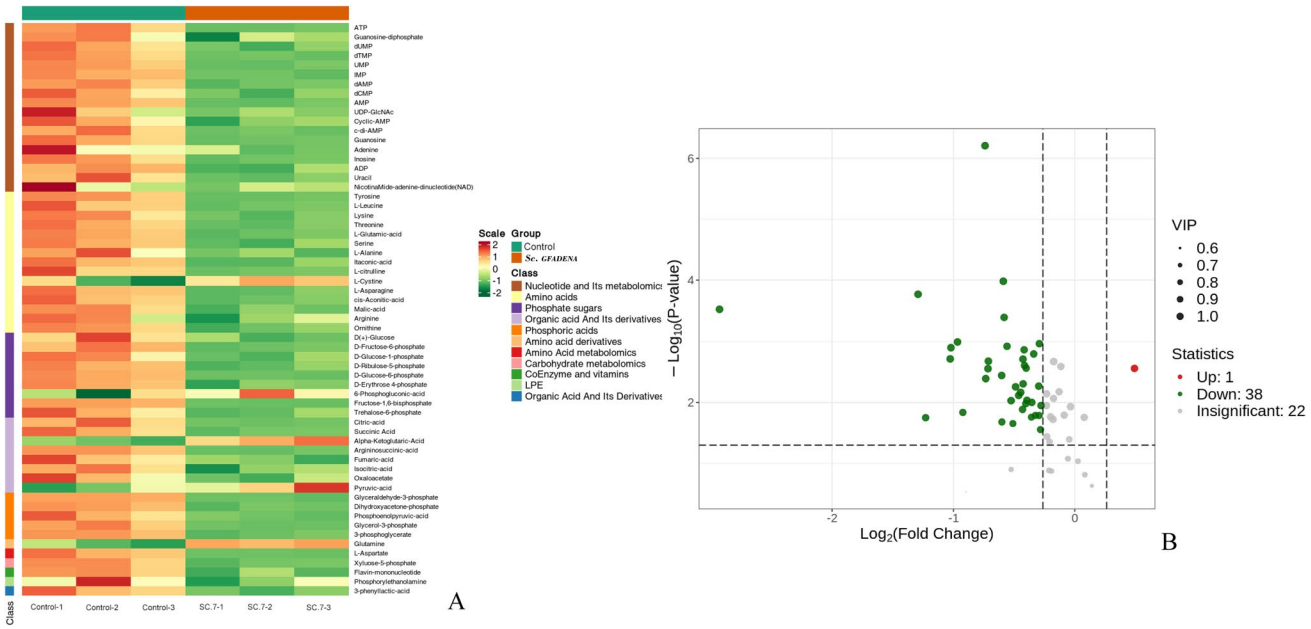

Fig. 5 Differential metabolites between *S. cerevisiae GFADENA* and the wild-type strain. Note: **A** Classification analysis of metabolites; **B** statistics analysis of significantly regulated metabolites based on the OPLS-DA model

6-phosphogluconic acid, *α*-ketogluconic acid, pyruvic acid, and glutamine in *S. cerevisiae GFADENA* exhibited an upward trend compared with the control group according to the expression contents. The contents of other metabolites in *S. cerevisiae GFADENA* exhibited a downward trend. In total, 39 differential metabolites in *S. cerevisiae GFADENA* were distinguished among all the metabolites according to the OPLS-DA model with *VIP* value > 1 and fold change ≥ 1.2. The volcano plot analysis represented that 38 significantly downregulated metabolites in *S. cerevisiae GFADENA* were distinguished (Fig. 5B). In all metabolites, *α*-ketogluconic acid (α-KG) was one of the significantly upregulated metabolites according to the OPLS-DA analysis. α-KG served as an energy donor, a precursor of amino acid biosynthesis, and an epigenetic regulator. α-KG also played physiological functions in immune regulation, oxidative stress, and anti-aging. The upregulation of α-KG in *S. cerevisiae GFADENA* provided an important basis for improving the tolerance of engineering strain. In addition, the downregulated metabolites were amino acids, such as *L*-aspartic acid, tyrosine, threonine, and *L*-glutamic acid, as well as sugars including *D* (+)—glucose, *D*-fructose-6-phosphate, *D*-glucose-1-phosphate, *D*-ribose-5-phosphate, and *D*-glucose-6-phosphate. The significantly differential metabolites from *S. cerevisiae GFADENA* after gene deletion were distinguished by the targeted metabolomics of energy metabolism.

Upregulated and downregulated metabolites of *S. cerevisiae* GFADENA

The dynamic distribution profiles of the top 5 upregulated and top 10 downregulated metabolites of *S. cerevisiae GFADENA* were drawn based on energy metabolism (Fig. 6A). The upregulated metabolites of *S. cerevisiae Sc*.7 were *L*-cystine, 6-phosphogluconic acid, α-ketogluconic acid, pyruvic acid, and glutamine, while the top 10 downregulated metabolites were *D*-fructose, glyceraldehyde-3 phase, NAD, *D*-glucose-1-phase, IMP, AMP, argininosuccinic acid, phosphoenolpyruvic acid, 3-phosphoglycerate, and fructose-1,6-bisphosphate. The maximum $\log_2$FC value was from *α*-ketogluconic acid (0.49), which was only one upregulated metabolite classified as data greater than 0. In addition, the minimum $\log_2$FC value was from fructose-1,6-bisphosphate (−2.93) with the most significant difference among all the downregulated metabolites (Fig. 6B).

KEGG annotation of *S. cerevisiae* GFADENA based on energy metabolism

Metabolism, environmental information processing, and genetic information processing were classified according to KEGG annotation of metabolomics of energy metabolism based on cell functions (Fig. 6C). The classification numbers of metabolism were much more than others based on functionality. Metabolic pathway function was the highest

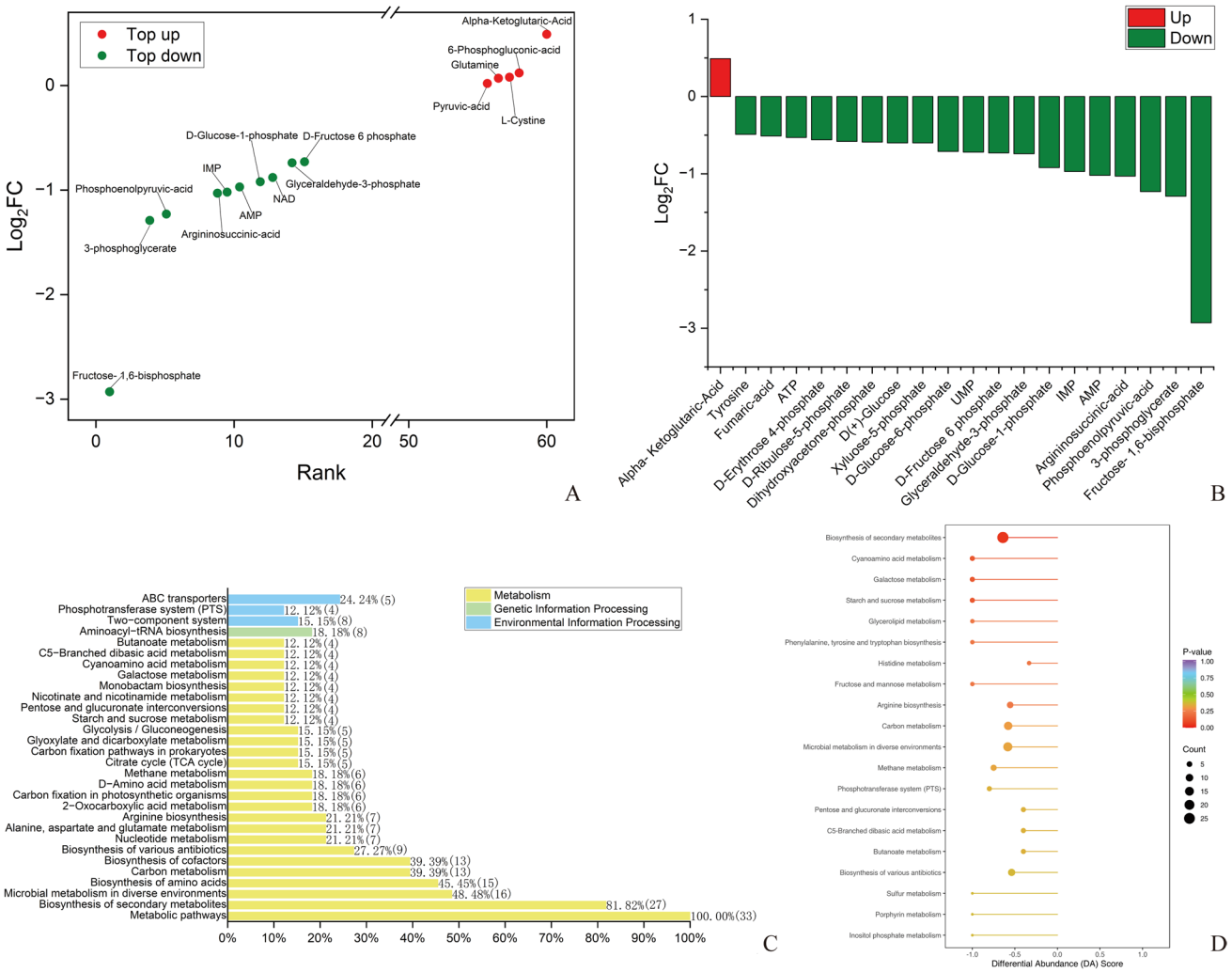

Fig. 6 Distribution and KEGG annotation of top-upregulated and downregulated metabolites in *S. cerevisiae GFADENA* based on energy metabolism. Note: **A** Dynamic distribution map of top metabolites; **B** log_2FC values of top-upregulated and downregulated metabolites. **C** The cell functions were classified based on the metabolomics of energy metabolism; **D** the distribution of 20 classified metabolisms based on the differential abundance scores

percentage among all the differentially significant metabolites. The biosynthesis percentages of secondary metabolites pathway, microbial metabolism in diverse environments, and amino acids functions accounted for 81.82%, 48.48%, and 45.45%, respectively. The percentages of ABC transporters, phosphotransferase system, and two-component system based on environmental information processing classification accounted for 23.4%, 12.12%, and 15.15%, respectively. The percentage of aminoacyl-tRNA biosynthesis accounted for 18.18% of genetic information processing classification.

The distribution profiles of *p*-values and counts of 20 classified metabolisms were provided according to the differential abundance (DA) scores of metabolisms (Fig. 6D). The biosynthesis of secondary metabolites had the highest count value based on a DA score of − 0.5 among all the metabolisms. Other metabolisms with a DA score of − 1.0 were from cyanoamino acid metabolism, galactose metabolism, starch and sucrose metabolism, and fructose and mannose metabolism. Thus, the deletion of seven genes resulted in the regulation of metabolites in *S. cerevisiae GFADENA* involving metabolism, environmental information processing, and genetic information processing based on energy metabolism.

Targeted metabolomics of amino acid metabolism of *S. cerevisiae* GFADENA

The determination data of index, compounds, and class based on the amino acid sigMetabolites of targeted metabolomics are listed in Table S2. The distribution profiles of ten top-upregulated and four top-downregulated metabolites were represented according to log_2FC values of metabolites based on amino acid metabolism in *S. cerevisiae*

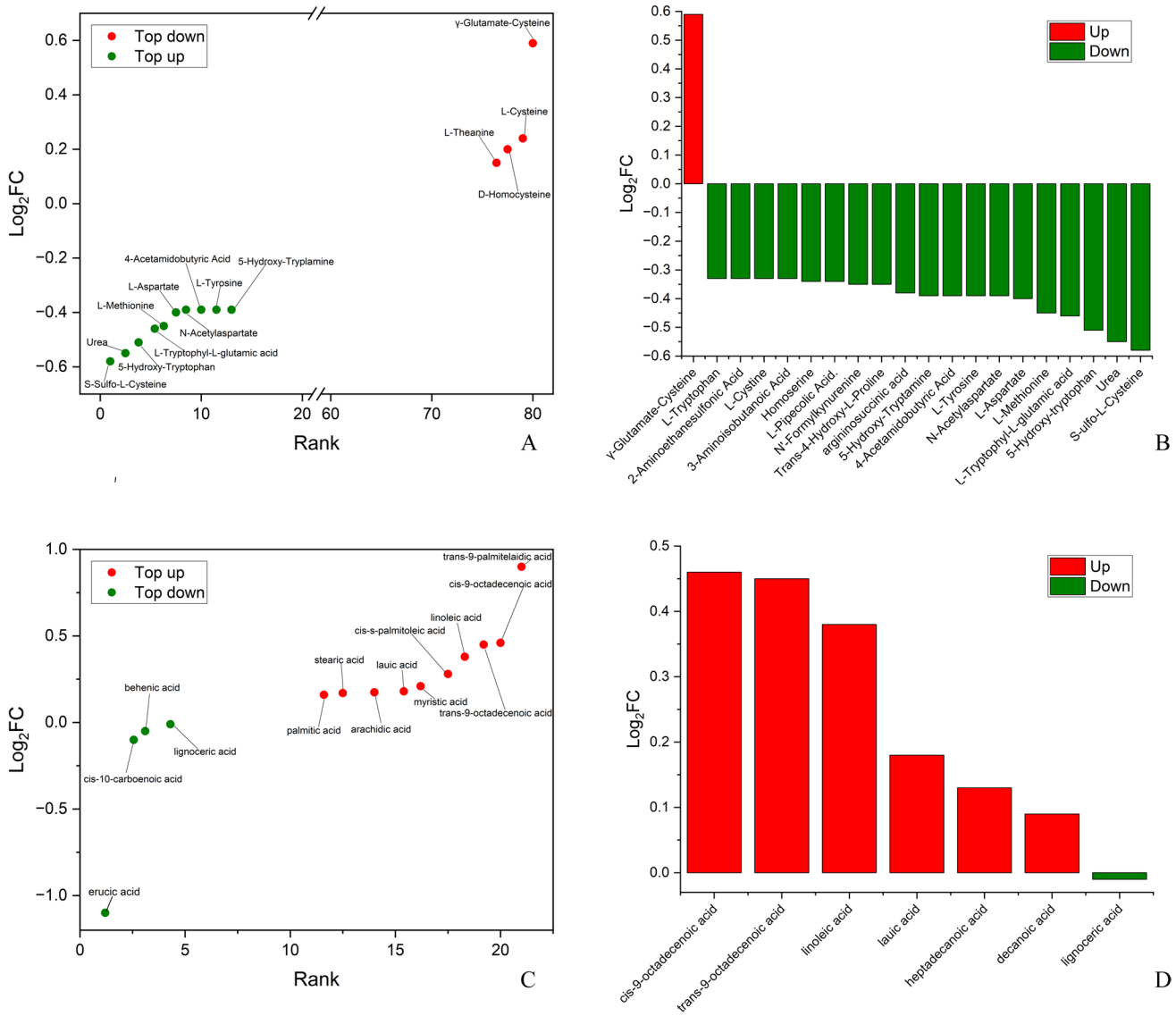

Fig. 7 Distribution of top-upregulated and downregulated metabolites in *S. cerevisiae GFADENA* based on the amino acid and free fatty acid metabolisms. Note: **A** The dynamic distribution map of top metabolites based on the amino acid metabolism; **B** log_2FC values of top metabolites based on the amino acid metabolism; **C** the dynamic distribution map of top metabolites based on the free fatty acid metabolism; **D** the log_2FC values of top metabolites based on the free fatty acid metabolism

GFADENA (Fig. 7A). Top-upregulated metabolites were from *γ*-glutamate-cysteine, *L*-cysteine, *D*-homocysteine, and *L*-theanine. The top-downregulated metabolites were from *L*-aspartate, 4-acetamido butyric acid *L*-tyrosine, 5-hydroxy-tryptamine, *N*-acetylaspartate, *L*-methionine, *L*-tryptophyl-*L*-glutamic acid, 5-hydroxy-tryptophan, urea, and *S*-sulfo-*L*-cysteine. The highest log_2FC value from upregulated metabolite *γ*-glutamate-cysteine was 0.58 with the biggest value among the 20 top metabolites (Fig. 7B). In addition, top-downregulated metabolites (log_2FC values) were from *S*-sulfo-*L*-cysteine (−0.58), urea (−0.55), and 5-hydroxy-tryptophan (−0.51). Thus, the deletion of seven genes in *S. cerevisiae GFADENA* resulted in upregulated and downregulated metabolites according to the targeted metabolomics based on amino acid metabolism.

Targeted metabolomics of free fatty acid metabolism

The determination data of index, compounds, and class from free fatty acid sigMetabolites based on the targeted metabolomics are listed in Table S3. The distribution profiles of ten top-upregulated and four top-downregulated metabolites were drawn based on free fatty acid metabolism (Fig. 7C). The ten top-upregulated metabolites were from trans-9-palmitelaidic acid, cis-9-octadecenoic acid,

trans-9-octadecenoic acid, cis-s-palmitoleic acid, myristic acid, lauric acid, linoleic acid, arachidic acid, stearic acid, and palmitic acid. In addition, the downregulated metabolites were from cis-10-carbonic acid, behenic acid, lignoceric acid, and erucic acid. The $\log_2$FC values of top metabolites were represented in terms of differential fold changes (Fig. 7D). The upregulated metabolites with the largest fold changes were from cis-9-octadecenoic acid (0.46), trans-9-octadecenoic acid (0.45), linoleic acid (0.37), lignoceric acid (0.18), heptadecanoic acid (0.13), and decanoic acid (0.09). In addition, one downregulated differential metabolite was from lignoceric acid (−0.02). Therefore, the gene deletion in *S. cerevisiae GFADENA* resulted in upregulated and downregulated metabolites of free fatty acids based on the targeted metabolomics.

Discussion

S. cerevisiae was generally exposed to stress and inhibition under high-concentration sucrose conditions in breadmaking and sucrose ethanol (Ando et al. 2006). Despite its importance, the development of *S. cerevisiae* with high-stress tolerance to sucrose was still not given enough attention. Various approaches including mutation breeding and fermentation processes of viable yeast cell numbers, time consumption, and sucrose utilization have been explored and developed to enhance stress tolerance (Ando et al. 2006). *S. cerevisiae* could produce 4.5% (w/v) of ethanol after 72 h of fermentation using the fermentation of 250 g/L of sucrose concentration with 130 g/L sucrose (Breisha 2010). The high-concentration sucrose inhibited yeast growth under high osmotic pressure. In this study, each gene deletion of *GPD2*, *FPS1*, *ADH2*, *DLD3*, *ERG5*, *NTH1*, and *AMS1* exhibited different phenotypes due to the function of the metabolism in yeast cells. The deletion of *GPD2*, *FPS1*, *ADH2*, and *DLD3* resulted in the increase of ethanol yield by reducing byproduct formation and inhibiting byproduct transport. The deletion of *ERG5*, *NTH1*, and *AMS1* caused the tolerance enhancement to sucrose by regulating the oligosaccharides formation in the yeast cell membrane. This study integrated the specific advantages of the tested genes to achieve high ethanol yield and high sucrose tolerance. *S. cerevisiae GFADENA* after the deletion of *GPD2*, *FPS1*, *ADH2*, *DLD3*, *ERG5*, *NTH1*, and *AMS1* obtained its high tolerance to sucrose under the high-concentration condition. The ethanol concentration of *S. cerevisiae GFADENA* was 1.17 folds compared to the wild-type strain using 400 g/L sucrose. Specifically, in the initial cultivation stage, *S. cerevisiae GFADENA* had faster cell proliferation than the wild-type strain. In addition, *S. cerevisiae GFADENA* could produce ethanol with the highest concentration of 145 g/L using 400 g/L of corn syrup. The utilization rate of corn syrup reached 97%. *S. cerevisiae GFADENA* possessed excellent characteristics of high-sugar tolerance improvement and conversion rate enhancement.

The improvement of excellent traits in yeast involving high-sugar tolerance and sugar-ethanol conversion rate enhancement required systemic metabolic regulation involving multiple genes (van Aalst et al. 2022). The modification of a single specific gene could regulate yeast's traits. *POG1* gene deletion in baker's yeast drastically enhanced the fermentation ability after freeze–thaw stress in bread dough (Sasano et al. 2013). The overexpression of baker's yeast *SNR84* improved stress tolerance with 98% higher cell viability using 300 g/L of sucrose (Lin et al. 2015). However, the high-quality yeast needed to modify multiple traits involving systematic regulation by more genes. The single-gene modification was undoubtedly inadequate for practical needs. In this study, the deletion of *GPD2*, *FPS1*, *ADH2*, and *DLD3* genes contributed to ethanol production improvement by reshaping the metabolic pathway from glucose to ethanol. *ERG5*, *NTH1*, and *AMS1* deletion in *S. cerevisiae GFADENA* resulted in the enhancement of cellular rigidity and flexibility by increasing the fecosterol, trehalose, and mannan contents in yeast's cell wall. This study further indicated that multiple-gene modification was an effective approach to predetermined performance enhancement based on rational design.

The comprehensive omics approach unveiled the molecular mechanism by comparing genomes or transcriptomes with the advent of high-throughput detection technology (Park et al. 2005). The phenotype difference of engineering strain after gene modification provided important clues to facilitate rational modification for further improvement (Hong et al. 2010). The interventions of post-transcriptional and protein post-translational regulations affected the information flow between gene and phenotype (Putri et al. 2013). In addition, genomics or transcriptomics is reflected in the final phenotype based on the differences at the gene or transcript levels (Hirasawa et al. 2006). To comprehensively unveil the molecular mechanism of intracellular metabolites, technological metabolomics interrogated the cell closer to the phenotype (Rochfort 2005). Metabolites unlike transcripts and proteins were regarded as the ultimate responses to environmental or genetic changes as the end cellular products in the regulatory processes (Fukusaki and Kobayashi 2005). Thus, the link between phenotype and metabolome was direct to interventions because the metabolome changes represented a high correlation with the objective phenotype.

In this study, energy, amino acid, and free fatty acid metabolisms were performed to unveil the molecular mechanisms by analyzing the correlation between phenotype and metabolome. α-Ketoglutaric acid and fructose-1,6-bisphosphate in *S. cerevisiae GFADENA* based on energy metabolism were the most significantly different

upregulation and downregulation metabolites, respectively ($p < 0.05$). The stress tolerance enhancement and ethanol production increase of *S. cerevisiae GFADENA* were related to the regulation of metabolites involving metabolism, environmental information processing, and genetic information processing according to the targeted energy metabolomics. However, further exploration was needed to address the ethanol yield increase and stress tolerance enhancement by certain specific genes in *S. cerevisiae*. The response surface methodology was used to optimize key factors like temperature, pH, and dissolved oxygen to enhance ethanol production (Arora et al. 2015). In addition, the reduced dynamic flux balance model using artificial neural networks was also an alternative method to improve the ethanol yield in terms of accuracy and computational time of available experimental data (Eslamloueyan and Setoodeh 2011). Further, immobilizing yeast cells on the carrier could increase ethanol yield and ethanol productivity in an immobilized cell reactor (Yan et al. 2012).

The CRISPR-Cas9 system enabled the precise modification of the yeast genome by altering a 20-nucleotide sequence using the guide RNA expression vectors. However, the CRISPR-Cas9 system had several limitations mainly including off-target effects, epigenetics, and mitochondrial editing (Sato and Kuroda 2023). The gRNA bonded to non-target sequences was similar to the target sequence. Off-target effects caused double-strand breaks in the non-target region (Hsu et al. 2013; Mali et al. 2013). In addition, the Cas9 protein could not change the epigenetic state of the target sequence. The Cas9/gRNA complex recruitment was inhibited by the epigenetic state. The chemical modification affected gene expression and chromatin condensation states (Nicoglou and Merlin 2017). The epigenetic differences were frequently linked to important cell phenotypes (Cavalli and Heard 2019). Further, the CRISPR-Cas9 system targeted DNA in the cell nucleus. The potential editing targets also existed in mitochondria and chloroplasts (Tuppen et al. 2010). Cas9 protein was transported to mitochondria via the fusion of the mitochondrial targeting sequence. However, the mechanism of polynucleotide transportation to the mitochondria was still unclear (Loutre et al. 2018). The CRISPR-Cas9 methods would be improved to address the current limitations by the integration of cutting-edge genome editing and extend to broader cellular processes (Shaw et al. 2019; Zhang et al. 2022).

Supplementary Information The online version contains supplementary material available at https://doi.org/10.1007/s00253-025-13446-w.

Author contribution All the authors contribute to the study conceptualization and design. P.Z.Y. conceived the study idea and paper proposal, analyzed data, and wrote the manuscript. J.Q.F. contributed to new reagents or analytical tools. J.C.C. conducted experiments**.** All the authors have read and agreed to the published version of the manuscript.

Funding This study was supported by the Hefei Municipal Natural Science Foundation (2022047).

Data availability The raw data supporting the conclusions of this article will be made available by the authors, without undue reservation. Data for the targeted metabolomics were provided in the supplementary files in this manuscript.

Declarations

Ethics approval This article does not contain any studies with human participants or animals performed by any of the authors.

Consent to participate Not applicable.

Consent for publication Not applicable.

Competing interest The authors declare no competing interests.

References

Ando A, Tanaka F, Murata Y, Takagi H, Shima J (2006) Identification and classification of genes required for tolerance to high-sucrose stress revealed by genome-wide screening of *Saccharomyces cerevisiae*. FEMS Yeast Res 6(2):249–267. https://doi.org/10.1111/j.1567-1364.2006.00035.x

Arora R, Behera S, Sharma NK, Kumar S (2015) A new search for thermotolerant yeasts, its characterization and optimization using response surface methodology for ethanol production. Front Microbiol 6:16. https://doi.org/10.3389/fmicb.2015.00889

Beese-Sims SE, Lee J, Levin DE (2011) Yeast Fps1 glycerol facilitator functions as a homotetramer. Yeast 28(12):815–819. https://doi.org/10.1002/yea.1908

Breisha GZ (2010) Production of 16% ethanol from 35% sucrose. Biomass Bioenerg 34(8):1243–1249. https://doi.org/10.1016/j.biombioe.2010.03.017

Caspeta L, Chen Y, Ghiaci P, Feizi A, Buskov S, Hallstrom B, Petranovic D, Nielsen J (2014) Altered sterol composition renders yeast thermotolerant. Science 346(6205):75–78. https://doi.org/10.1126/science.1258137

Cavalli G, Heard E (2019) Advances in epigenetics link genetics to the environment and disease. Nature 571(7766):489–499. https://doi.org/10.1038/s41586-019-1411-0

Crowe JH, Carpenter JF, Crowe LM (1998) The role of vitrification in anhydrobiosis. Annu Rev Physiol 60:73–103. https://doi.org/10.1146/annurev.physiol.60.1.73

El-Sheekh M, Bedaiwy M, El-Nagar A, ElKelawy M, Bastawissi H (2022) Ethanol biofuel production and characteristics optimization from wheat straw hydrolysate: performance and emission study of dI- diesel engine fueled with diesel/biodiesel/ethanol blends. Renew Energy 191:591–607. https://doi.org/10.1016/j.renene.2022.04.076

Eslamloueyan R, Setoodeh P (2011) Optimization of fed-batch recombinant yeast fermentation for ethanol production using a reduced dynamic flux balance model based on artificial neural networks. Chem Eng Commun 198(11):1309–1338. https://doi.org/10.1080/00986445.2011.560512

Flemming HC, Wingender J (2010) The biofilm matrix. Nat Rev Microbiol 8(9):623–633. https://doi.org/10.1038/nrmicro2415

Fukusaki E, Kobayashi A (2005) Plant meta-bolomics: potential for practical operation. J Biosci Bioeng 100(4):347–354. https://doi.org/10.1263/jbb.100.347

Gietz RD, Schiestl RH (2007) Large-scale high-efficiency yeast transformation using the LiAc/SS carrier DNA/PEG method. Nat Protoc 2(1):38–41. https://doi.org/10.1038/nprot.2007.15

Girelli CR, Papadia P, Pagano F, Miglietta PP, Fanizzi FP, Cardinale M, Rustioni L (2023) Metabolomic NMR analysis and organoleptic perceptions of pomegranate wines: influence of cultivar and yeast on the product characteristics. Heliyon 9(6):1–10. https://doi.org/10.1016/j.heliyon.2023.e16774

Gold ND, Gowen CM, Lussier FX, Cautha SC, Mahadevan R, Martin VJJ (2015) Metabolic engineering of a tyrosine-overproducing yeast platform using targeted metabolomics. Microb Cell Fact 14:1–9. https://doi.org/10.1186/s12934-015-0252-2

Gombert AK, van Maris AJA (2015) Improving conversion yield of fermentable sugars into fuel ethanol in 1st generation yeast-based production processes. Curr Opin Biotechnol 33:81–86. https://doi.org/10.1016/j.copbio.2014.12.012

Hirasawa T, Nakakura Y, Yoshikawa K, Ashitani K, Nagahisa K, Furusawa C, Katakura Y, Shimizu H, Shioya S (2006) Comparative analysis of transcriptional responses to saline stress in the laboratory and brewing strains of with DNA microarray. Appl Microbiol Biot 70(3):346–357. https://doi.org/10.1007/s00253-005-0192-6

Hirayama H, Suzuki T (2011) Metabolism of free oligosaccharides is facilitated in the *och1δ* mutant of *Saccharomyces cerevisiae*. Glycobiology 21(10):1341–1348. https://doi.org/10.1093/glycob/cwr073

Hong M-ELK-S, Yu BJ, Sung Y-J, Park SM, Koo HM, Kweon D-H, Park JC, Jin Y-S (2010) Identification of gene targets eliciting improved alcohol tolerance in *Saccharomyces cerevisiae* through inverse metabolic engineering. J Biotechnol 149:52–59

Hsu PD, Scott DA, Weinstein JA, Ran FA, Konermann S, Agarwala V, Li YQ, Fine EJ, Wu XB, Shalem O, Cradick TJ, Marraffini LA, Bao G, Zhang F (2013) DNA targeting specificity of RNA-guided Cas9 nucleases. Nat Biotechnol 31(9):827. https://doi.org/10.1038/nbt.2647

Hubmann G, Guillouet S, Nevoigt E (2011) Gpd1 and Gpd2 fine-tuning for sustainable reduction of glycerol formation in *Saccharomyces cerevisiae*. Appl Environ Microb 77(17):5857–5867. https://doi.org/10.1128/aem.05338-11

Kim I, Yun H, Jin I (2007) Comparative proteomic analyses of the yeast *Saccharomyces cerevisiae* KNU5377 strain against menadione-induced oxidative stress. J Microbiol Biotechnol 17(2):207–217

Kim HS, Kim NR, Yang J, Choi W (2011) Identification of novel genes responsible for ethanol and/or thermotolerance by transposon mutagenesis in *Saccharomyces cerevisiae*. Appl Microbiol Biot 91(4):1159–1172. https://doi.org/10.1007/s00253-011-3298-z

Lam F, Ghaderi A, Fink G, Stephanopoulos G (2014) Engineering alcohol tolerance in yeast. Science 346(6205):71–75. https://doi.org/10.1126/science.1257859

Lin X, Zhang CY, Bai XW, Feng B, Xiao DG (2015) Improvement of stress tolerance and leavening ability under multiple baking-associated stress conditions by overexpression of the *SNR84* gene in baker's yeast. Int J Food Microbiol 197:15–21. https://doi.org/10.1016/j.ijfoodmicro.2014.12.014

Loutre R, Heckel AM, Smirnova A, Entelis N, Tarassov I (2018) Can mitochondrial DNA be CRISPRized: *Pro* and *Contra*. IUBMB Life 70(12):1233–1239. https://doi.org/10.1002/iub.1919

Mali P, Yang LH, Esvelt KM, Aach J, Guell M, DiCarlo JE, Norville JE, Church GM (2013) RNA-guided human genome engineering *via* Cas9. Science 339(6121):823–826. https://doi.org/10.1126/science.1232033

Marques WL, Raghavendran V, Stambuk BU, Gombert AK (2016) Sucrose and *Saccharomyces cerevisiae*: a relationship most sweet. FEMS Yeast Res 16(1):1–8. https://doi.org/10.1093/femsyr/fov107

Montague TG, Cruz JM, Gagnon JA, Church GM, Valen E (2014) CHOPCHOP: a CRISPR/Cas9 and TALEN web tool for genome editing. Nucleic Acids Res 42(W1):W401–W407. https://doi.org/10.1093/nar/gku410

Nicoglou A, Merlin F (2017) Epigenetics: a way to bridge the gap between biological fields. Stud Hist Philos Sci Part C-Stud Hist Philos Biol Biomed Sci 66:73–82. https://doi.org/10.1016/j.shpsc.2017.10.002

Nwaka S, Kopp M, Holzer H (1995) Expression and function of the trehalase genes *NTH1* and *YBR0106* in *Saccharomyces cerevisiae*. J Biol Chem 270(17):10193–10198. https://doi.org/10.1074/jbc.270.17.10193

Park SJ, Lee SY, Cho J, Kim TY, Lee JW, Park JH, Han MJ (2005) Global physiological understanding and metabolic engineering of microorganisms based on omics studies. Appl Microbiol Biot 68(5):567–579. https://doi.org/10.1007/s00253-005-0081-z

Putri SP, Nakayama Y, Matsuda F, Uchikata T, Kobayashi S, Matsubara A, Fukusaki E (2013) Current metabolomics: practical applications. J Biosci Bioeng 115(6):579–589. https://doi.org/10.1016/j.jbiosc.2012.12.007

Randez-Gil F, Sanz P, Prieto JA (1999) Engineering baker's yeast: room for improvement. Trends Biotechnol 17(6):237–244. https://doi.org/10.1016/s0167-7799(99)01318-9

Rochfort S (2005) Metabolomics reviewed: a new "Omics" platform technology for systems biology and implications for natural products research. J Nat Prod 68(12):1813–1820. https://doi.org/10.1021/np050255w

Sasano Y, Haitani Y, Hashida K, Oshiro S, Shima J, Takagi H (2013) Improvement of fermentation ability under baking-associated stress conditions by altering the *POG1* gene expression in baker's yeast. Int J Food Microbiol 165(3):241–245. https://doi.org/10.1016/j.ijfoodmicro.2013.05.015

Sato G, Kuroda K (2023) Overcoming the limitations of CRISPR-Cas9 systems in *Saccharomyces cerevisiae*: off-target effects, epigenome, and mitochondrial editing. Microorganisms 11(4):19. https://doi.org/10.3390/microorganisms11041040

Shaw WM, Yamauchi H, Mead J, Gowers GOF, Bell DJ, Öling D, Larsson N, Wigglesworth M, Ladds G, Ellis T (2019) Engineering a model cell for rational tuning of GPCR signaling. Cell 177(3):782. https://doi.org/10.1016/j.cell.2019.02.023

Trimble RB, Atkinson PH (1992) Structural heterogeneity in the Man8-13GlcNAc oligosaccharides from log-phase *Saccharomyces* yeast: a one- and two-dimensional ^{1}H NMR spectroscopic study. Glycobiology 2(1):57–75. https://doi.org/10.1093/glycob/2.1.57

Tuppen HAL, Blakely EL, Turnbull DM, Taylor RW (2010) Mitochondrial DNA mutations and human disease. Biochim Biophys

Acta-Bioenerg 1797(2):113–128. https://doi.org/10.1016/j.bbabio.2009.09.005

Umekawa M, Ujihara M, Makishima K, Yamamoto S, Takematsu H, Wakayama M (2016) The signaling pathways underlying starvation-induced upregulation of α-mannosidase *Ams1* in *Saccharomyces cerevisiae*. Biochim Biophys Acta 1860(6):1192–1201. https://doi.org/10.1016/j.bbagen.2016.02.018

van Aalst ACA, de Valk SC, van Gulik WM, Jansen MLA, Pronk JT, Mans R (2022) Pathway engineering strategies for improved product yield in yeast-based industrial ethanol production. Synth Syst Biotechnol 7(1):554–566. https://doi.org/10.1016/j.synbio.2021.12.010

Verstrepen KJ, Iserentant D, Malcorps P, Derdelinckx G, Van Dijck P, Winderickx J, Pretorius IS, Thevelein JM, Delvaux FR (2004) Glucose and sucrose: hazardous fast-food for industrial yeast? Trends Biotechnol 22(10):531–537. https://doi.org/10.1016/j.tibtech.2004.08.001

Wang Z, Zhang LY, Tan TW (2010) High cell density fermentation of *Saccharomyces cerevisiae* GS2 for selenium-enriched yeast production. Korean J Chem Eng 27(6):1836–1840. https://doi.org/10.1007/s11814-010-0300-x

Wu L, Wen YD, Chen WY, Yan TS, Tian XF, Zhou SS (2021) Simultaneously deleting *ADH2* and *THI3* genes of *Saccharomyces cerevisiae* for reducing the yield of acetaldehyde and fusel alcohols. Fems Microbiol Lett 368(15):1–8. https://doi.org/10.1093/femsle/fnab094

Wu CY, Liu L, Zhang MM, Jike X, Zhang HX, Yang NA, Yang HR, Xu HD, Lei HJ (2023) Mechanisms of antioxidant dpeptides enhancing ethanol-oxidation cross-stress tolerance in lager yeast: roles of the cell wall and membrane. J Agr Food Chem 1–11. https://doi.org/10.1021/acs.jafc.3c03793

Yan SB, Chen XS, Wu JY, Wang PC (2012) Ethanol production from concentrated food waste hydrolysates with yeast cells immobilized on corn stalk. Appl Microbiol Biotechnol 94(3):829–838. https://doi.org/10.1007/s00253-012-3990-7

Yang P, Wu W, Chen J, Jiang S, Zheng Z, Deng Y, Lu J, Wang H, Zhou Y, Geng Y, Wang K (2023) Thermotolerance improvement of engineered *Saccharomyces cerevisiae ERG5 Delta ERG4 Delta ERG3 Delta*, molecular mechanism, and its application in corn ethanol production. Biotechnol Biofuels Bioproducts 16(1):1–9. https://doi.org/10.1186/s13068-023-02312-4

Zhang J, Hansen LG, Gudich O, Viehrig K, Lassen LMM, Schrübbers L, Adhikari KB, Rubaszka P, Carrasquer-Alvarez E, Chen L, D'Ambrosio V, Lehka B, Haidar AK, Nallapareddy S, Giannakou K, Laloux M, Arsovska D, Jorgensen MAK, Chan LJG, Kristensen M, Christensen HB, Sudarsan S, Stander EA, Baidoo E, Petzold CJ, Wulff T, O'Connor SE, Courdavault V, Jensen MK, Keasling JD (2022) A microbial supply chain for production of the anti-cancer drug vinblastine. Nature 609(7926):341. https://doi.org/10.1038/s41586-022-05157-3